Applied Mathematics and Computation 265 (2015) 1026–1043

Contents lists available at ScienceDirect

Applied Mathematics and Computation

journal homepage: www.elsevier.com/locate/amc

The stochastic SEIR model before extinction: Computational approaches

J.R. Artalejo [a], A. Economou [b,*], M.J. Lopez-Herrero [c]

[a] Department of Statistics and Operations Research, Faculty of Mathematics, Complutense University of Madrid, 28040 Madrid, Spain
[b] Department of Mathematics, University of Athens, Panepistemiopolis, 15784 Athens, Greece
[c] Faculty of Statistical Studies, Complutense University of Madrid, 28040 Madrid, Spain

ARTICLE INFO

Keywords:
Stochastic SEIR epidemic model
Extinction time
Ratio-of-expectations distribution

ABSTRACT

We study a stochastic epidemic model of Susceptible-Exposed-Infective-Removed (SEIR) type and we quantify its behavior during an outbreak. More specifically, we model the epidemic by a continuous-time Markov chain and we develop efficient computational procedures for the distribution of the duration of an outbreak. We also study the evolution of the epidemic before its extinction using the ratio-of-expectations (RE) distribution for the number of individuals in the various classes of the model. The obtained results are illustrated by numerical examples including an application to an outbreak of Marburg hemorrhagic fever.

© 2015 Elsevier Inc. All rights reserved.

1. Introduction

The fundamental epidemic model for the study of the spread of an epidemic disease that confers immunity is the Susceptible-Infective-Removed (SIR) that was initially studied in depth in the pioneering paper of Kermack and McKendrick [34]. According to this model, the individuals of a population are classified as susceptible (S – if previously unexposed to the pathogen), infective (I – if currently colonized by the pathogen) or removed (R – if they have cleared the infection). In its initial version, the model concerns a closed population of N individuals and the dynamics of the state $(S(t), I(t), R(t))$ of the system, that records the numbers of individuals in the various classes, is governed by a system of ordinary differential equations (ODEs).

One drawback of the SIR model is that it assumes that after the transmission of the disease to a susceptible individual, the individual becomes immediately infective. However, the process of transmission occurs in most cases with an initial transfer of a very small number of bacterial cells or viruses. Thus, for a period of time the pathogen abundance is too low in the tagged individual for active transmission to other susceptible individuals. During this period the individual is in some sense infected but not yet infective (latent period). Such an individual is referred to as exposed (E). Similarly to the SIR model, when N is large, the population can be represented by a deterministic Susceptible-Exposed-Infective-Removed (SEIR) model of ODEs, where the independent variable is the time and the dependent variables refer to the number of individuals in the various classes S, E , I and R. More accurately, this deterministic model is an appropriate limit of the corresponding stochastic version that we study in some detail below. The relation between a deterministic epidemic model and its stochastic counterparts has been studied excessively in the literature, since it is an issue of great theoretical and practical significance (see e.g. Bartlett [12], Jacquez and Simon [31] and Allen and Allen [3]). In the present case, the system of ODEs describing the dynamics of an SEIR epidemic model has the

* Corresponding author. Tel.: +30 6945257505.
E-mail addresses: jesus_artalejo@mat.ucm.es (J.R. Artalejo), aeconom@math.uoa.gr (A. Economou), lherrero@estad.ucm.es (M.J. Lopez-Herrero).

http://dx.doi.org/10.1016/j.amc.2015.05.141
0096-3003/© 2015 Elsevier Inc. All rights reserved.

following form:

$$\begin{aligned}\frac{dS}{dt} &= -\frac{\beta}{N}IS,\\ \frac{dE}{dt} &= \frac{\beta}{N}IS - \sigma E,\\ \frac{dI}{dt} &= \sigma E - \gamma I,\\ \frac{dR}{dt} &= \gamma I,\end{aligned} \tag{1}$$

where β is the contact-infection rate per pair of $S-I$ individuals, σ is the rate at which an exposed individual becomes infective, γ is the recovery rate, and $S(t)+E(t)+I(t)+R(t)=N$, for every $t \geq 0$ (since the population is considered closed).

The above deterministic SEIR model and its generalizations have received a lot of attention from various researchers [20,32,35,37,38,42]. Indeed, the SEIR model represents more accurately the spread of an epidemic than the corresponding SIR model that does not take into account the latent period. The SEIR model has a slower growth rate, since after the pathogen invasion the susceptible individuals need to pass through the exposed class before they can contribute to the transmission process.

For a small population size N, the adoption of a stochastic model is more appropriate than a deterministic approach [2,4,15,17,33]. For the case of the fundamental SIR model there is a huge literature dealing with stochastic (Markovian) models. A crucial difference with the deterministic model is that the associated Markov chain is almost surely (with probability 1) absorbed in some state where the number of infectives is 0, within finite time. As a result, the stationary distribution of the number of individuals in the various classes is concentrated on the set of absorbing states. In this sense, it is interesting to study distributions that quantify the behavior of the epidemic before its extinction. One possibility is the use of the so-called quasi-stationary distribution [18,48]. Practically speaking, the quasi-stationary distribution of a Markov chain that describes the evolution of an epidemic is the conditional limiting distribution of the state of the population, as time goes to infinity, given that the extinction of the epidemic has not yet occurred. The importance of the quasi-stationary distribution depends on the type of the disease being considered. For epidemic dynamics that confer immunity, the usefulness of quasi-stationarity is rather limited. Indeed, in such cases there is no endemic situation and the quasi-stationary distribution is of no practical use. It is only when the corresponding deterministic model has a stable endemic point, that the quasi-stationary distribution is of interest because the stochastic model will then fluctuate around this 'equilibrium' for a long time before it eventually reaches the absorbing extinction state.

Another possibility for the quantification of an epidemic before its extinction is the use of the so-called Ratio-of-Expectations (RE) distribution and its variants [8,11,18]. In a sense, the RE-distribution gives the 'mean' fractions of time that a population spends in the various states till the extinction of the epidemic. In other words, its value at a certain state is the expected time that the process spends in this state till the extinction of the epidemic, divided by the expected duration of the epidemic. The notion of the RE-distribution goes back at least to the seminal paper of Darroch and Seneta [19] (see Section 3) who discuss it in relationship with the notion of the quasi-stationary distribution of an absorbing Markov chain, though they do not use a specific name for it. On the other hand, one approach to model the quasi-stationary regime is to imagine that the absorbing Markov chain is returned to an initial transient state at some small rate ϵ, every time that the absorption (i.e., the extinction) occurs. The stationary distribution of this 'returned' process that has been called also pseudo-transient distribution (see Ewens [22]) is also related to the RE-distribution. For a comparative study for the quasi-stationary and RE-distributions, we refer to the paper by Artalejo and Lopez-Herrero [8].

The computation of the moments of the extinction time in the context of stochastic epidemic models has been studied by a significant number of authors that have provided important theoretical insight and computational formulas [25,41,44]. However, the related problem of the computation of the whole distribution of the extinction time has received less attention (for some recent results in the framework of SIS and SIR stochastic epidemic models see [6,7]).

In the case of the SEIR model, the number of papers that assume a stochastic point of view is quite small. Svensson [45] considered a stochastic multi-compartment epidemic model, where an individual passes from the susceptible to the removed state through a number of intermediate infectious states that are characterized by different infectivity capacities. His model includes the stochastic SEIR model as a special case. Svensson [45] proved an asymptotic expression for the extinction time in a stochastic SEIR model with respect to the population size N. Swinton [46] extended this study to spatially structured stochastic SEIR models. Grasman [27] considered the SEIR model with demography and proposed an efficient method for the quantification of its long-term stochastic dynamics. Recently, several authors have proceeded in the quantification of more involved stochastic models of SEIR type which encompass intervention policies such as vaccination and isolation [10,43]. However, it is fair to say that the focus of most papers on stochastic SEIR models is on theoretical asymptotic results with respect to the population size (central limit theorems) and on phase-transition phenomena (i.e., on drastic changes in the behavior of the models when a parameter exceeds some threshold value). Another thread of the stochastic–statistical research on the subject deals with the fitting of SEIR models in real data and its implications, using statistical methods and simulation [16,26,28,29].

The objective of the present paper is to complement these studies by proposing efficient computational methodologies for the quantification of the behavior of stochastic SEIR models. Our methodology pertains to the numerical analysis point of view for quantifying a stochastic model, i.e. we derive some equations that govern the evolution of the model and we solve them by developing efficient numerical methods. Another way to tackle the same problem is to use stochastic simulation, i.e. to generate

multiple possible trajectories of the stochastic model and derive an approximation of the performance measures of interest, by considering their corresponding sample averages. This latter methodology, that goes back at least to the fundamental work of Gillespie [23,24], constitutes another thread of research for the quantification of analytically intractable stochastic epidemic models.

In contrast to most previous studies, we are interested in the computation of the distributions of interest and not only on their moments. Moreover, we seek for exact results that are applicable for small and moderate values of the population size N (as it is typical for the stochastic approach) and not for asymptotic results as $N \to \infty$. More specifically, in the present paper we consider the basic stochastic SEIR model that relates directly to the deterministic counterpart (1) and we propose computational procedures for the quantification of the system dynamics. We concentrate on the following points:

- We develop a recursive scheme for the computation of the probability mass function that corresponds to the RE-distribution of an epidemic. The RE-distribution quantifies the behavior of the epidemic before its extinction, by giving the fractions of time that the process spends in the various states till the extinction of the epidemic. In the present case, where the quasi-stationary distribution is degenerate, it provides an informative alternative.
- We obtain numerically stable recursive schemes for the computation of the Laplace–Stieltjes transforms (LSTs) and the moments of any order of the remaining duration of the epidemic given its current state.

Using the aforementioned computational procedures, we have performed a large number of computational experiments. In particular, we have tested our approach against Gillespie's algorithm and we have seen that it outperforms simulations, for small and moderate population sizes, where the stochastic approach is more applicable. Moreover, we have performed an extensive sensitivity analysis of the stochastic SEIR model to identify which parameters are most important in determining the model output. This effort enhances the understanding of the disease dynamics and determines which aspects in the system are good targets for a possible intervention.

A summary description of the more insightful findings derived from our results is as follows:

- The RE-distribution provides a valuable quantification of the epidemic as long as the infection process is still active.
- Long latent periods slow the disease spreading. Therefore, the time to extinction can drastically increase.
- The time to extinction may not be an increasing function of the contact-infection rate. Thus, intervention and control strategies could give false indications, if they are based on a reduction of the time to extinction.
- The extinction time distribution and the RE-distribution may exhibit a bimodal shape.
- There exist simple formulas relating the expected final size, the expected time to extinction and the RE expected values of the individuals in the E and I classes.

The rest of the paper is organized as follows. In Section 2, we first introduce the mathematical formulation of the stochastic SEIR model as a continuous-time Markov chain X. In Section 3, we develop an algorithmic recursive scheme for the computation of the LSTs and the moments of the time to reach any state of the underlying Markov chain starting from a fixed initial state. We then apply this scheme for the computation of the RE-distribution. In Section 4, we focus on the distribution of the extinction time. The implementation of the theoretical results and the sensitivity analysis are carried out in Section 5. This section also includes our numerical experiments for the Marburg fever 2005 outbreak in Angola. We conclude with some comments and some problems for future research in Section 6. Some auxiliary results are presented in the Appendices: the block structure of the infinitesimal generator of X (Appendix A) and a method for the symbolic inversion of the conditional LSTs of the extinction time (Appendix B).

2. The stochastic SEIR model

In this section, we describe the stochastic epidemic model that relates directly to the deterministic counterpart (1). Let us consider a closed population of N individuals and a contagious disease that has a latent period and that confers immunity. Every individual of the population at a given time is classified as susceptible, exposed, infective or removed. The incubation periods for the exposed individuals (i.e., the periods where the individuals have contacted the disease but they are not yet infective) are assumed to be independent and identically distributed according to an exponential distribution with rate σ. Similarly, the infectious periods of different infectives are independent exponentially distributed random variables with rate γ. During his/her infectious period an infective makes contacts with any given individual at the time points of a time homogeneous Poisson process with intensity $\frac{\beta}{N}$. If a contacted individual is still susceptible, then he/she becomes exposed, but he is able to infect other individuals only after his incubation period has been completed, whence he/she becomes infective. After the completion of the infectious period, an individual is considered 'removed' and plays no further role in the epidemic spread. The epidemic ceases as soon as there are no more infectious nor exposed individuals in the population. All Poisson processes, incubation and infectious periods are assumed independent. Then, the stochastic SEIR model is a continuous-time 3-dimensional Markov chain $X = \{(S(t), E(t), I(t)) : t \geq 0\}$, that records the number of susceptible, exposed and infective individuals at any time point. There is no need to record the number of removed individuals, since it can be immediately determined by $R(t) = N - S(t) - E(t) - I(t)$.

We suppose that the epidemic begins with one infective individual that is inserted in a totally susceptible population; that is, the initial state of X is $(S(0), E(0), I(0)) = (N-1, 0, 1)$. Then, we can easily see that the state space of X is $S = S_1 - S_2$, where $S_1 = \{(s, e, i) : 0 \leq s, e, i \leq N,\ s + e + i \leq N\}$ and $S_2 = \{(s, e, 0) : 0 \leq s, e \leq N,\ s + e = N\}$. The infection ends when $E(t) = I(t) = 0$

so the set of the absorbing states is $S_A = \{(s, 0, 0) : 0 \le s \le N-1\}$. Since the set of transient states $S_T = S - S_A$ is a finite set, absorption occurs in a finite time with probability 1. Regarding the cardinality of the state space, we observe that $|S| = |S_1| - |S_2| = \binom{4+N-1}{N} - \binom{2+N-1}{N} = \frac{N(N+1)(N+5)}{6}$.

The exponential transition rates of the Markov chain X are given by

$$q_{(s,e,i)(s',e',i')} = \begin{cases} \beta_{si}, & \text{if } (s',e',i') = (s-1, e+1, i), \\ \sigma_e, & \text{if } (s',e',i') = (s, e-1, i+1), \\ \gamma_i, & \text{if } (s',e',i') = (s, e, i-1), \\ -q_{sei}, & \text{if } (s',e',i') = (s, e, i), \\ 0, & \text{otherwise,} \end{cases} \tag{2}$$

where $\beta_{si} = \frac{\beta}{N} si$, $\sigma_e = \sigma e$, $\gamma_i = \gamma i$ and $q_{sei} = \beta_{si} + \sigma_e + \gamma_i$, for $(s, e, i) \in S$.

In Appendix A, we show that the infinitesimal generator $\mathbf{Q}$ of X has a block triangular representation, which guarantees that the numerical implementation of the epidemic indicators is stable.

The matrix structure of the infinitesimal generator $\mathbf{Q}$ and the definition of the levels in Appendix A suggest that we order the states $(s, e, i) \in S$ in the natural class order; that is, they are sorted first with respect to the number of susceptible individuals s, then with respect to the number of exposed individuals e and finally with respect to the number of infective individuals i, for $0 \le s \le N-1$, $0 \le e \le N-s-1$ and $0 \le i \le N-s-e$.

Once the state ordering is fixed, we see that the sub-generator $\mathbf{Q}_T$ associated with the set of transient states S_T is a lower triangular matrix. Thus, we can easily see, using the results in van Doorn and Pollett [47], that the quasi-stationary distribution assigns all its probability mass to one or two states (to (0, 0, 1) for $\gamma \le \sigma$ and to (0, 1, 0), (0, 0, 1) for $\gamma > \sigma$), i.e. it is almost degenerate. This is due to the fact that the SEIR model is non-endemic. Therefore, we will consider the RE-distribution as a measure of practical relevance for the quantification of the epidemic before its extinction.

3. The RE distribution

In this section, we develop an algorithmic procedure for the computation of the RE-distribution of the stochastic SEIR model. More concretely, the RE distribution is obtained by generalizing a methodology introduced by Neuts and Li [40] for the numerical implementation of the final size distribution in the stochastic SIR model. The generalization provides a recursive approach to compute distributions and moments for the times to reach various states of the process X, starting from the initial state $(s_0, e_0, i_0) = (N-1, 0, 1)$.

Let L_{sei} be the first-passage time to $(s, e, i) \in S$. Moreover, we define

$$\begin{aligned} \phi_{sei}(z) &= E[e^{-zL_{sei}} 1_{\{L_{sei}<\infty\}}], \ Re(z) \ge 0, \\ \theta_{sei} &= \Pr[L_{sei} < \infty], \\ m^{(l)}_{sei} &= E[L^l_{sei} 1_{\{L_{sei}<\infty\}}], \ l \ge 0, \end{aligned}$$

where 1_E denotes the indicator random variable of an event E.

For a fixed state $(s, e, i) \in S$, we consider those states (s', e', i') that are possibly last visited just before the epidemic reaches the state (s, e, i). More concretely, starting from $(s_0, e_0, i_0) = (N-1, 0, 1)$, the state (s, e, i) is reachable only through three states: *i*) $(s+1, e-1, i)$ (if $i \ne 0$, $e \ne 0$, $s \ne N-1$), or *ii*) $(s, e+1, i-1)$ (if $i \ne 0$ and $e \ne N-s-1$) or *iii*) $(s, e, i+1)$ (if $i \ne N-s-e$). Then, the time L_{sei} is decomposed as $L_{s'e'i'} + T_{(s',e',i')(s,e,i)}$, where $T_{(s',e',i')(s,e,i)}$ denotes the transition time from (s', e', i') to (s, e, i). Thus, we obtain the following stable algorithm that governs the LSTs dynamics. For convenience in the notation, we use Kronecker's delta symbol δ_{xy} which is defined to be 1, when $x = y$, and it equals 0 otherwise.

Algorithm 1. The conditional LSTs $\phi_{sei}(z)$ of the times to reach the various states $(s, e, i) \in S$, given that the initial state is $(N-1, 0, 1)$, are computed by using the following recursive scheme:

Step 1: Set

$$\phi_{N-1,01}(z) = 1, \ \phi_{N-1,00}(z) = \frac{\gamma_1}{z + q_{N-1,01}}. \tag{3}$$

Step 2a: Set $s = N-2$.
Step 2b: Set $e = N-s-1$.
Step 2c: Set $i = N-s-e$.
Step 2d: Set

$$\begin{aligned} \phi_{sei}(z) = {} & (1-\delta_{i0})(1-\delta_{e0}) \frac{\beta_{s+1,i}}{z + q_{s+1,e-1,i}} \phi_{s+1,e-1,i}(z) + (1-\delta_{i0})(1-\delta_{e,N-s-1}) \frac{\sigma_{e+1}}{z + q_{s,e+1,i-1}} \phi_{s,e+1,i-1}(z) \\ & + (1-\delta_{i,N-s-e}) \frac{\gamma_{i+1}}{z + q_{se,i+1}} \phi_{se,i+1}(z). \end{aligned} \tag{4}$$

Step 3a: Set $i = i-1$. If $i \ge 0$, then go to Step 2d.
Step 3b: Set $e = e-1$. If $e \ge 0$, then go to Step 2c.

Step 3c: Set $s = s - 1$. If $s \geq 0$, then go to Step 2b.

By differentiating $l \geq 1$ times the LSTs (3) and (4) with regard to z and setting $z = 0$, we can obtain a system of linear equations for the moments of order l, $m_{sei}^{(l)}$, in terms of moments of smaller order. The derivation follows from routine algebra so we omit this here.

Given the initial state $(s_0, e_0, i_0) = (N-1, 0, 1)$, the RE-distribution of the stochastic SEIR epidemic model is defined by the ratio

$$p_{sei}^{RE} = \frac{E_{(N-1,01)}[T_{sei}]}{E_{(N-1,01)}[L(\infty)]}, \ (s, e, i) \in S_T,$$

where T_{sei} is the time that the Markov chain X spends in state $(s, e, i) \in S_T$ before absorption.

In other words, p_{sei}^{RE} is the expected time that the process X spends in state (s, e, i) until the extinction of the epidemic divided by the expected duration of the epidemic. So, in some sense, p_{sei}^{RE} quantifies the fraction of time that X spends in state (s, e, i) until absorption. We recall that each state is visited at most once. In such a case, the expected time in state (s, e, i) is $1/q_{sei} = (\beta_{si} + \sigma_e + \gamma_i)^{-1}$. Thus, we conclude with the following result.

Theorem 1. *The RE-distribution* $\mathbf{p}^{RE} = (p_{sei}^{RE} : (s, e, i) \in S_T)$ *is given by*

$$p_{sei}^{RE} = \frac{\frac{\theta_{sei}}{\beta_{si}+\sigma_e+\gamma_i}}{\sum_{(s',e',i')\in S_T} \frac{\theta_{s'e'i'}}{\beta_{s'i'}+\sigma_{e'}+\gamma_{i'}}}, \ (s, e, i) \in S_T,$$

where θ_{sei}, *for* $(s, e, i) \in S_T$, *are computed from Algorithm 1.*

The expected values corresponding to the RE-distributions of the number of individuals E_{RE} and I_{RE} in the E and I classes quantify intuitively the mean number of exposed and infected individuals during an outbreak of the epidemic. They are related to the expected values of the final size $R(\infty)$ and the extinction time $L(\infty)$ through the relationships

$$E_{(s_0,e_0,i_0)}[E_{RE}] = \frac{E_{(s_0,e_0,i_0)}[R(\infty)] - i_0}{E_{(s_0,e_0,i_0)}[L(\infty)]} \times \frac{1}{\sigma}, \tag{5}$$

$$E_{(s_0,e_0,i_0)}[I_{RE}] = \frac{E_{(s_0,e_0,i_0)}[R(\infty)]}{E_{(s_0,e_0,i_0)}[L(\infty)]} \times \frac{1}{\gamma}. \tag{6}$$

The validity of the above expressions follows from Little's law (see e.g. [36]). Little's law has been originally stated in the framework of Queueing theory (see [39]) and states that the mean number of units in an input–output stochastic system is equal to the mean arrival rate of units, multiplied by the mean sojourn time of a unit in the system. In the present framework, the first factors in the right-hand sides of the formulas (5) and (6) can be respectively viewed as the arrival rates of individuals at the E and I classes during an outbreak, whereas $\frac{1}{\sigma}$ and $\frac{1}{\gamma}$ are the mean sojourn times of an individual in the corresponding classes. On the other hand, the left-hand sides of the formulas (5) and (6) are the mean number of units in the corresponding classes and therefore the equations are valid in the light of Little's law.

The recursive procedure of Algorithm 1 can be used for obtaining also the final size distribution of the model. Indeed, by using the algorithm for $l = 0$, setting $z = 0$, we obtain the probabilities $\theta_{sei} = \phi_{sei}(0)$ to reach the various states $(s, e, i) \in S$, given that the initial state is $(N-1, 0, 1)$. Then, the probability that the final size is n is just $\theta_{N-n,00}$, for $1 \leq n \leq N$. However, it is well known that the final size distributions of the stochastic SEIR and the corresponding SIR model coincide and can be calculated using the embedded jump chain (see e.g. Ball [9], Daley and Gani [17] or Andersson and Britton [4], Theorem 2.2 for the classical results, Black and Ross [14] for a new methodology and House et al. [30] for a recent survey). This happens because long latent periods cause delays in the transmission chain $S \to E \to I$, but do not change the potential risk at which one marked susceptible individual is exposed. The numerical implementation of our algorithm for the final size distribution shows that our approach provides the same results with the existing approaches. Thus, we do not elaborate further on this issue.

4. The distribution of the extinction time

The extinction time of the SEIR epidemic is the absorption time of X in $S_A = \{(s, 0, 0) : 0 \leq s \leq N-1\}$. If the initial state is $(N-1, 0, 1)$, then the LST $\phi_{L(\infty)}(z)$ of the extinction time can be computed as

$$\phi_{L(\infty)}(z) = \sum_{s=0}^{N-1} \phi_{s00}(z),$$

where $\phi_{s00}(z)$ are determined by appealing to Algorithm 1.

However, for a thorough quantification of the duration of an epidemic, it is more informative that we also compute the characteristics of the extinction time (i.e., LSTs and moments) starting from all various transient states. This enables us to update easily our estimates for the duration and the impact of the epidemic and to propose intervention measures, given that we observe

dynamically its evolution. Having this objective in mind, we present here a recursive scheme that provides the conditional LSTs of the duration of the epidemic, starting from all possible transient states.

To this end, let Λ_{sei} be the time to reach the set of absorbing states S_A, starting from a state $(s, e, i) \in S$. We also define

$$\varphi_{sei}(z) = E[e^{-z\Lambda_{sei}}],\ Re(z) \geq 0,$$
$$\vartheta_{sei} = \Pr[\Lambda_{sei} < \infty],$$
$$\mu_{sei}^{(l)} = E[\Lambda_{sei}^{l}],\ l \geq 0.$$

Notice that the submatrix that corresponds to the set of transient states is a triangular matrix with non-null diagonal elements (see Appendix A), so it is invertible (see e.g. Theorem 1.7.1 in [5]) and consequently the probability of extinction of the epidemic is 1. Therefore, $\vartheta_{sei} = 1$, for $(s, e, i) \in S$.

We now observe that $\Lambda_{sei} = 0$ and $\varphi_{sei}(z) = 1$, for $(s, e, i) \in S_A$. Otherwise, we use a first-step argument [36]; that is, we condition on the first state visited by X, after the completion of the exponential sojourn time in (s, e, i), to obtain a recursive relation that gives $\varphi_{sei}(z)$ in terms of $\varphi_{s-1,e+1,i}(z)$, $\varphi_{s,e-1,i+1}(z)$ and $\varphi_{se,i-1}(z)$. Using this relation, we can compute $\varphi_{sei}(z)$, for the successive states (s, e, i) in the natural order described in Section 3.

The recursive scheme is summarized in the following Algorithm 2.

Algorithm 2. The conditional LSTs $\varphi_{sei}(z)$ of the extinction time, for $(s, e, i) \in S$, are computed by using the following recursive scheme:

Step 1: Set

$$\varphi_{000}(z) = \cdots = \varphi_{N-1,00}(z) = 1. \tag{7}$$

Step 2a: Set $s = 0$.
Step 2b: Set $e = 0$.
Step 2c: Set $i = \delta_{e0}$.
Step 2d: Set

$$\varphi_{sei}(z) = (1-\delta_{i0})(1-\delta_{s0})\frac{\beta_{si}}{z+q_{sei}}\varphi_{s-1,e+1,i}(z) + (1-\delta_{e0})\frac{\sigma_e}{z+q_{sei}}\varphi_{s,e-1,i+1}(z) + (1-\delta_{i0})\frac{\gamma_i}{z+q_{sei}}\varphi_{se,i-1}(z). \tag{8}$$

Step 3a: Set $i = i + 1$. If $i \leq N - s - e$, then go to Step 2d.
Step 3b: Set $e = e + 1$. If $e \leq N - s - 1$, then go to Step 2c.
Step 3c: Set $s = s + 1$. If $s \leq N - 1$, then go to Step 2b.

For $0 \leq s \leq N - 1$ and $l \geq 1$, Eq. (7) gives immediately

$$\mu_{s00}^{(l)} = 0. \tag{9}$$

On the other hand, by multiplying Eq. (8) by $z + q_{sei}$, differentiating l times and evaluating at 0, we obtain equations for the moments $\mu_{sei}^{(l)}$. In particular, we have

$$\mu_{sei}^{(l)} = (1-\delta_{i0})(1-\delta_{s0})\frac{\beta_{si}}{q_{sei}}\mu_{s-1,e+1,i}^{(l)} + (1-\delta_{e0})\frac{\sigma_e}{q_{sei}}\mu_{s,e-1,i+1}^{(l)} + (1-\delta_{i0})\frac{\gamma_i}{q_{sei}}\mu_{se,i-1}^{(l)} + \frac{l}{q_{sei}}\mu_{sei}^{(l-1)}. \tag{10}$$

The recursive computations of the moments $\mu_{sei}^{(l)}$, up to any desired order l, is then a minor variant of Algorithm 2, with (7) and (8) replaced by (9) and (10), respectively. Note that the recursive Eq. (10) contains only conditional moments of one order less, which is convenient for minimizing the required computer storage space.

When one is interested in computing probabilities associated to the extinction time of the SEIR epidemic (e.g., survival probabilities or distribution functions), it is necessary to deal with the probability density function of the extinction time Λ_{sei}. In our numerical experiments, we have used the widely adopted algorithms developed by Abate and Whitt [1] for the numerical inversion of LSTs obtained in Algorithm 2. However, we note that the symbolic inversion of the LSTs is possible and it can be shown that the probability density functions can be decomposed to linear combinations of exponential and Erlang probability density functions. We provide some details in Appendix B. Since the associated algorithmic scheme is quite complicated and prone to numerical instability, we do not pursue its implementation in this paper.

5. Numerical experiments

In this section, we present several numerical results from the implementation of the algorithms developed so far, for the quantification of the stochastic SEIR model. We have articulated the exposition of our numerical experiments in three parts. In the first part, we present results regarding the comparison of our approach with simulation. In the second part, we carry our an extensive sensitivity analysis of the main descriptors of the stochastic SEIR model with respect to the various epidemic parameters. Finally, in the third part, we deal with the outbreak of Marburg fever that occurred in Angola in 2005. This epidemic has been studied originally using a deterministic SEIR model [13]. We supplement this study by showing some implications of the stochastic approach.

Table 1
CPU times comparison (in seconds).

	$N = 50$	$N = 100$	$N = 250$	$N = 500$	$N = 600$	$N = 1000$
Numerical	0.1093	0.8125	18.3750	226.6563	433.6875	3087.7970
Simulation	8.0937	24.3437	101.5469	261.2031	328.6406	645.5156

5.1. Comparison of the numerical algorithms with simulations

In this subsection we report some findings regarding the performance of our algorithms in comparison to stochastic simulation. In particular, we have compared our approach with the classical Gillespie's discrete event simulation algorithm (see e.g. [50]). This discrete event simulation algorithm generates trajectories of a stochastic process, by simulating times and types of events. In a Markovian framework, each transition of the underlying process involves the generation of two random numbers, one that gives the time for next transition and a second that provides the type of the next transition (e.g., to which state the process goes next).

In our comparison experiments, we have implemented Gillespie's algorithm to generate trajectories of the evolution of the epidemic process till its extinction and have registered the corresponding durations of the outbreaks. More concretely, for each simulation run, we start with $N-1$ susceptible individuals and 1 infective and the run is terminated when the population contains neither infective nor exposed individuals (i.e., when the Markov chain enters in the set of absorbing states S_A).

By performing N_r simulation runs, we get a random sample of extinction times $(T_1, \cdots, T_{N_r})$ and we estimate the expected extinction time, $E[L(\infty)]$, by the corresponding sample mean $\overline{T} = N_r^{-1} \sum_{i=1}^{N_r} T_i$, which constitutes an unbiased estimator. The Central Limit Theorem ensures that $\overline{T}$ has approximately a normal $\mathcal{N}(E[L(\infty)], Var[L(\infty)]/N_r)$ distribution. As our numerical algorithms provide the values of $E[L(\infty)]$ and $Var[L(\infty)]$, we determine the sample size (i.e., the number of simulation runs) by controlling the half width of a 95% confidence interval for $\overline{T}$ to be at most 0.05. Therefore, the number of runs, N_r, for each simulation scenario is chosen as the ceiling of $Var[L(\infty)](1.96/0.05)^2$.

The numerical experiments have shown that, regarding accuracy, in any case, the largest differences between $E[L(\infty)]$, $Var[L(\infty)]$ and their sample counterparts were less than 0.03, showing that the differences were indeed within the sample error.

Regarding speed, we implemented both approaches in a personal computer of 2.31 GHz and 2 GB RAM. We compared the CPU times required to get $E[L(\infty)]$ and $Var[L(\infty)]$, using the numerical algorithms and Gillespie's algorithm, for various population sizes and model rates. The results depend strongly on the population size N and the other parameters of the model (in particular the rate σ).

In a scenario with model rates $\beta = 2.0$, $\gamma = 1.0$ and $\sigma = 0.5$, we varied the population size N. Results are collected in Table 1. Our numerical algorithm computed the mean durations of the epidemics in shorter CPU times than the simulation algorithm for $N \leq 540$. For larger population sizes, the simulation algorithm provides the results in shorter times. For instance, the CPU times associated to $N = 1000$ were 3087.7 s and 646.5 s for the numerical algorithm and Gillespie's algorithm respectively. But, it should be pointed here that our computational procedure gives, in a single run, extinction times from all transient states (notice that for $N = 1000$ the state space contains $1,676,67,500$ such states), while the simulation algorithm gives the mean duration of an outbreak only for the fixed starting state.

We also considered the effect of the model rates. For example, for a population of $N = 250$ individuals, latency rate $\sigma = 0.5$ and $\mathcal{R}_0 = \frac{\beta}{\gamma} > 1$, the CPU time for the numerical algorithm was 18 s, while the simulation algorithm took up to 100 s, to achieve the above mentioned accuracy. In general, as the latency rate σ goes to zero (i.e., larger incubation periods), the variance of the duration of an outbreak increases and to achieve a given accuracy, we have to run more simulation trajectories, so the numerical algorithm seems preferable.

In summary, the comparison of the numerical algorithms and the simulation approach leads to the following conclusions:

- For small and moderate population sizes, where the stochastic modeling is considered more appropriate than its deterministic counterpart, the numerical algorithms are faster than Gillespie's algorithm. For larger populations, simulation results in shorter CPU times.
- The numerical algorithm is much more efficient than simulation, when one is interested in computing the mean residual durations of an outbreak from any transient state. This is convenient for updating the predictions for the mean remaining duration of an outbreak, as the epidemic progresses, without performing further calculations.
- For epidemics with large incubation periods, the numerical algorithms seem more preferable than simulations, even for moderately large population sizes.

5.2. Sensitivity analysis of the stochastic SEIR model

In the numerical experiments of this subsection, we have set the mean recovery time $1/\gamma$ to be the time unit, i.e., $\gamma = 1.0$. Thus, for the basic reproduction ratio $\mathcal{R}_0$, which gives the expected number of secondary cases per primary case, we have that

Table 2
Expected extinction time and standard deviation.

	$N = 25$	$N = 50$	$N = 100$	$N = 250$	$N = 500$	$N = 1000$
$\beta = 0.5$	2.36722	2.46590	2.52425	2.56367	2.57780	2.58509
	3.493927	3.729033	3.880885	3.991236	4.032808	4.054762
$\beta = 1.0$	4.47814	5.23366	5.98127	6.95673	7.68562	8.40779
	6.046854	7.465620	9.060901	11.469252	13.542934	15.859207
$\beta = 1.5$	6.86713	9.00666	11.75792	16.55293	20.82324	24.93191
	7.866301	10.663805	14.407845	21.064866	26.994750	32.603911
$\beta = 2.0$	8.77665	11.87518	15.45257	19.99597	22.95850	25.76035
	8.554611	11.579555	15.066441	19.375755	22.078106	24.674143
$\beta = 5.0$	10.52083	12.49516	14.37550	16.82617	18.67059	20.51180
	6.119678	6.882268	7.650622	8.726078	9.570465	10.432160
$\beta = 10.0$	9.79325	11.48409	13.16190	15.37078	17.03841	18.70464
	4.269076	4.676008	5.11681	5.735599	6.222963	6.722227

$\mathcal{R}_0 = \frac{\beta}{\gamma} = \beta$ and we will confirm the usual dichotomy on the behavior of the epidemic according to whether $\mathcal{R}_0 = \beta > 1$ or $\mathcal{R}_0 = \beta \leq 1$. For each experiment, we first describe the parameters of the model and the representation of the results (tables and figures). We then present our numerical findings with interpretations and conclusions.

5.2.1. Experiment 1: Mean value and standard deviation of the extinction time with respect to N *and* β

A. Parameters - Representation of the results. We consider a population size $N \in \{25, 50, 100, 250, 500, 1000\}$. In each case, the epidemic starts with a single infective inserted in an otherwise virgin population (i.e., the initial state is $(N-1, 0, 1)$). We consider various combinations of the main rates of the model; more specifically we have $\gamma = 1.0$, $\sigma = 0.5$, and $\beta \in \{0.5, 1.0, 1.5, 2.0, 5.0, 10.0\}$. The results are displayed in Table 2, where each cell contains two entries, the top one that corresponds to the expected value of the extinction time and the bottom entry that corresponds to the standard deviation. We notice that the values of interest can be efficiently computed, although the state space grows huge very quickly.

B. Numerical findings, interpretation and conclusions. A careful look on Table 2 reveals the following facts:

- For any fixed β, the expected duration of an outbreak (expected extinction time) and the standard deviation are increasing functions of the population size N.
- The effect of an increase on the population size on the expected duration of an outbreak and its standard deviation is very mild. This numerical finding agrees with the theoretical result of Svensson [45] who proved that asymptotically the extinction time is proportional to $\log N$ with a multiplicative constant that can be completely characterized by the parameters of the model.
- For any fixed N, the expected duration of an outbreak and its standard deviation are unimodal functions of β.

5.2.2. Experiment 2: Mean value and standard deviation of the extinction time with respect to σ *and* β

A. Parameters - Representation of the results. We consider a population of $N = 100$ individuals with a single infective individual, while the others are susceptible. The recovery rate is $\gamma = 1.0$ and we vary $\sigma \in (0, 10)$ and $\beta \in (0, 10)$. The results are displayed in Figs. 1 and 2 that are heat map style plots for the expected extinction time and its standard deviation respectively.

B. Numerical findings, interpretation and conclusions. Figs. 1 and 2 show the following facts:

- The expected duration of an outbreak and the standard deviation are unimodal functions of the contact-infection rate β. The maximum value for the expected length is located around $\beta = 2.5$ while the standard deviation presents a maximum around $\beta = 2.0$. Since the effect of an increase of β on the duration of an outbreak is ambiguous, we have performed an additional numerical experiment (see experiment 4) dealing with the whole distribution of the extinction time, with emphasis on modes and quantiles.
- Both the expected duration of an outbreak and its standard deviation are decreasing functions of the latency rate σ. When $\sigma \to \infty$, both measures tend to their corresponding quantities of the stochastic SIR model.

5.2.3. Experiment 3: Form of the extinction time distribution with respect to β *and the initial state of the epidemic.*

A. Parameters - Representation of the results. We consider, now, the whole distribution of the extinction time. In particular, we focus on the existence of a unique or multiple modes in its probability density function. To this end, we consider a population of $N = 100$ individuals and we assume that $\gamma = 1.0$ and $\sigma = 2.0$. In Fig. 3, we draw the probability density functions of the extinction time for $\beta \in \{1.0, 2.5, 5.0\}$, with initial state (98, 1, 0) for $\beta = 2.5$ and (99, 0, 1) for the other two choices of β.

B. Numerical findings, interpretation and conclusions. Fig. 3 suggests the following facts:

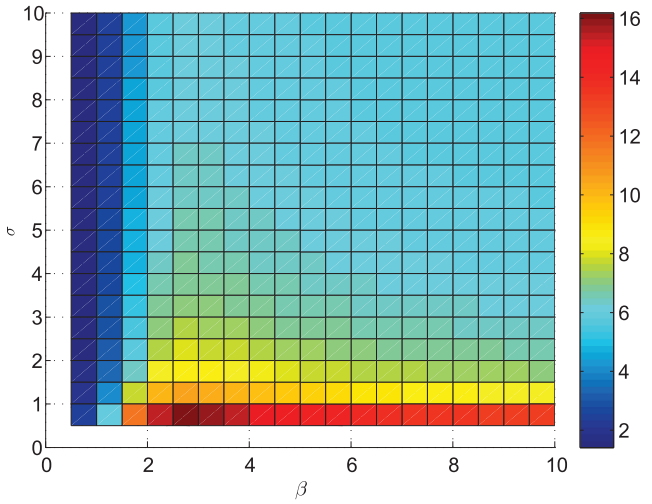

Fig. 1. Heat map plot for expected extinction time, $N = 100$.

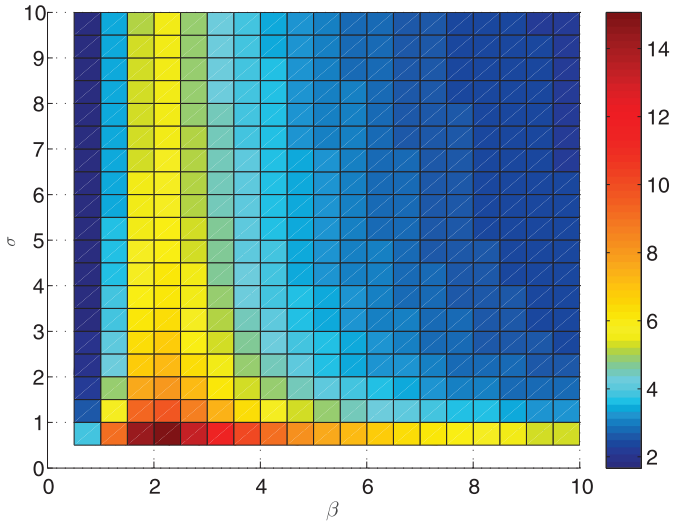

Fig. 2. Heat map plot for standard deviation of extinction time, $N = 100$.

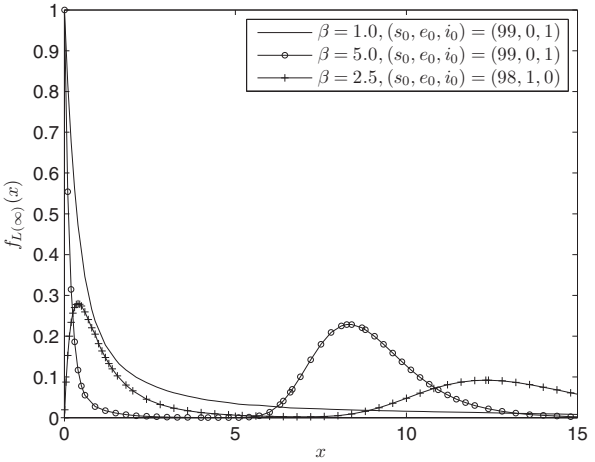

Fig. 3. Density functions of the extinction time.

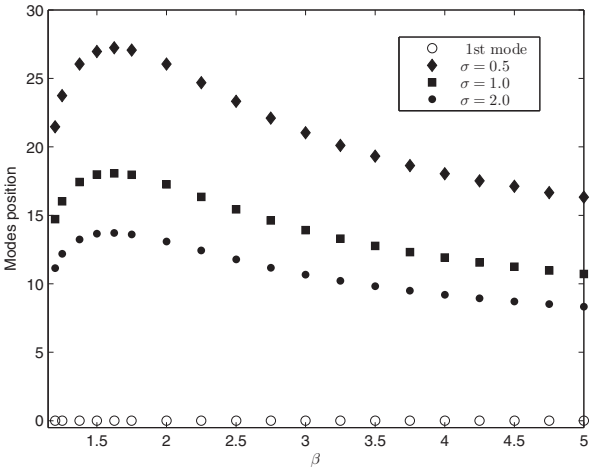

Fig. 4. Location of the modes. $N = 100$, $\gamma = 1.0$.

- The probability density function of the extinction time may be a decreasing, a unimodal or a bimodal function, depending on the magnitude of β and the initial state.
- A decreasing/unimodal shape of the probability density of the extinction time is associated with low values of β, when the epidemic dies out before spreading too much.
- A bimodal shape for the probability density of the extinction time is associated with an initial small number of individuals in the E and I classes and large values of β. Then, there is a chance that a minor epidemic occurs, but there is also a considerable chance that a major epidemic does occur.
- When the initial state is $(N-1, 0, 1)$, the probability density function of the extinction time has a mode at the origin, since the epidemic may die immediately if the unique infected individual is removed. In fact the value of the mode at the origin is γ. (This can be formally argued using a Tauberian result applied to the LST of the extinction time. Note that in the case of a continuous random variable, its LST coincides with the Laplace transform of its density. The Tauberian result states that the limit of a smooth function $F(t)$ at 0 can be obtained as the $\lim_{s\to\infty} s\mathcal{L}\{f\}(s)$, where $\mathcal{L}\{f\}(s)$ is the Laplace transform of $F(t)$ (see e.g. Dyke [21], Theorem 2.12)).
- When the initial state is not $(N-1, 0, 1)$, there is no chance for an immediate extinction of the epidemic; thus, the probability density function of the extinction time starts growing from the origin 0.

5.2.4. Experiment 4: Modes of the extinction time distribution with respect to σ and β.

A. Parameters - Representation of the results. We are now delving into the study of the modes of the probability density function of the extinction time, $L(\infty)$. We assume that the initial state is $(N-1, 0, 1)$. As we have commented earlier, in such cases, the probability density function of $L(\infty)$ has always a maximum at the origin. Moreover, when β varies, it presents either a decreasing shape (see curve for $\beta = 1.0$, in Fig. 3) or a bimodal shape (see curve for $\beta = 5.0$, in Fig. 3) with a first peak at zero. In the present experiment, we consider a population of $N = 100$ individuals, with $\gamma = 1.0$ and $\sigma \in \{0.5, 1.0, 2.0\}$. We vary β, for $\beta > 1$. Fig. 4 shows the location of the corresponding modes. Point marker plot, displayed over the x-axis, shows the first peak at the origin and the remainder three point plots give the positions of the second mode.

B. Numerical findings, interpretation and conclusions. Fig. 4 shows the following facts:

- As β surpasses 1, a second peak appears and moves quickly towards a maximum value. Then, it decreases slowly.
- The maximum distance between the two peaks appears when β is around 1.625.
- The latency rate σ plays a significant role in the location of the second peak, but not on the value of the contact-transmission rate β for which the peak occurs.
- There are two competing effects that affect the duration of an outbreak as β increases. On the one hand, the transmission potential of the epidemic increases ('positive' effect implying larger durations, as more individuals are infected), but on the other hand the synchronization of incidents increases ('negative' effect implying shorter durations, as most of the individuals are affected simultaneously).
- Preventive policies based on the decrease of the contact-transmission rate (such as isolation) may reduce the mean final size of an epidemic, but increase its mean duration.

5.2.5. Experiment 5: Box-plots of the extinction time distribution with respect to σ and β.

A. Parameters - Representation of the results. The above findings regarding the modes show that the expected duration of an outbreak is not an informative measure. The modes or its whole distribution are necessary for reliable predictions. In this experiment, we complement this point of view by studying the percentiles of the extinction time distribution. The results are

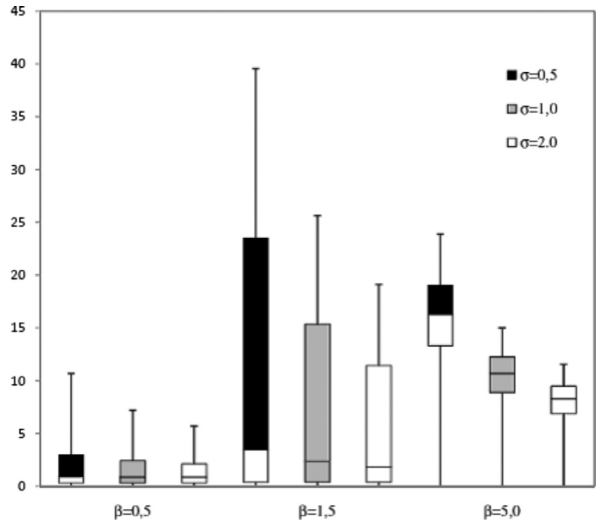

Fig. 5. Extinction time box plot diagram, $N = 100$.

presented in Fig. 5, which is a sort of box-plot diagram for the distribution of the extinction time. The bottom and the top of the box correspond to the first and third quartile respectively, whereas the band inside the box corresponds to the median (i.e., the second quartile). Down whisker always begins at 0 (the lowest possible value of the extinction time) and the end of the upper whisker gives the 95th percentile. Fig. 5 contains nine box-plots of this type, corresponding to combinations of the rates β and σ of the model in a population of $N = 100$ individuals, where the recovery rate is $\gamma = 1.0$. More specifically, we assume that $\beta \in \{0.5, 1.5, 5.0\}$ and $\sigma \in \{0.5, 1.0, 2.0\}$. From left to right, each group of three boxes corresponds to the same contact rate $\beta \in \{0.5, 1.5, 5.0\}$, respectively; within each group, boxes in black correspond to $\sigma = 0.5$, grey color boxes correspond to $\sigma = 1.0$ and white boxes represent $\sigma = 2.0$.

B. Numerical findings, interpretation and conclusions. The box-plot diagrams of Fig. 5 show a variety of shapes and behaviors of the corresponding extinction time distribution. In particular, we observe the following facts:

- For $\beta = 0.5$, the extinction time distribution is right skewed (in fact it presents a decreasing shape). Changes in the latency rate seem to have a minor effect on the duration of an outbreak.
- For $\beta = 1.5$, the lower 50%-percentile of the extinction time distribution, that is associated with the first mode at 0, shows less variability in comparison with the upper 50%-percentile that is associated with the second mode.
- For $\beta = 5.0$, the box-plot diagrams are almost symmetric with respect to the median, unlike the case where $\beta = 1.5$.
- An increase on the latency rate σ always implies a reduction of the length of the interquartile length of the duration of an outbreak.

5.2.6. Experiment 6: RE-distributions of the various classes of individuals.

A. Parameters - Representation of the results. We consider a population of $N = 500$ individuals with initial state (499, 0, 1) and parameters $\gamma = 1.0$ and $\beta = 2.0$. In Figs. 6 and 7, for $\sigma = 5.0$, we provide graphs of the RE probability mass functions for the R and S classes, respectively. In Fig. 8, we provide the RE distribution function for the E class, for $\sigma \in \{0.05, 1.0, 20.0\}$. Finally, in Fig. 9, we draw the expectations of the RE-distributions for the E and I classes, as functions of the latent rate σ.

B. Numerical findings, interpretation and conclusions. The following facts are inferred from the figures

- In Fig. 6, the RE probability mass function for the R class is bimodal. The first mode occurs at the origin, while a second proper mode is observed at 390. Other numerical results not reported here show that figures corresponding to other values of σ are very similar (i.e., the modes occur almost at the same points and the expected values are very close).
- The RE probability mass function for the S class plotted in Fig. 7 is also bimodal. Roughly speaking, its graph seems like the reflection (with respect to a vertical line) of the graph plotted in Fig. 6 for the R class. The transmission of individuals from the initial S class to the final R class explains the 'complementarity' observed in the figures.
- In Fig. 8, the RE distribution function of the number of exposed individuals is seen to increase with σ. This is explained, since the greater the rate σ, the shorter are the latent periods; therefore the fraction of time during an outbreak that the number of exposed individuals is below a certain level increases.
- Fig. 9 shows complementarity between the E and I classes. The RE expected value of exposed individuals decreases with σ, which agrees with the monotone behavior observed in Fig. 8. On the other hand, the RE expected value of the number of infectives is an increasing function of σ. The explanation follows from the Little's relationship (6) , if we recall that the expected time to extinction decreases with σ , while the final size does not depend on σ.

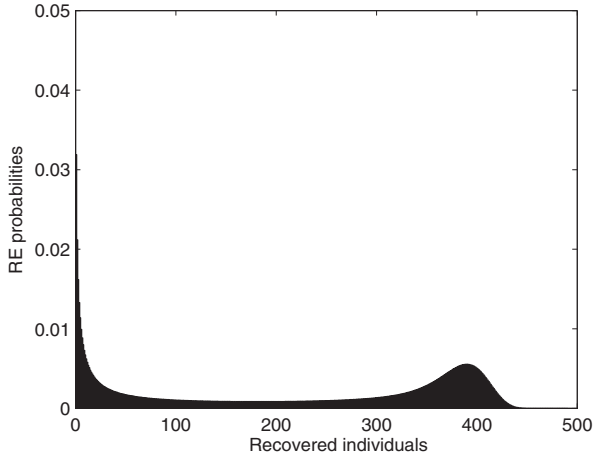

Fig. 6. RE mass function - *R* class.

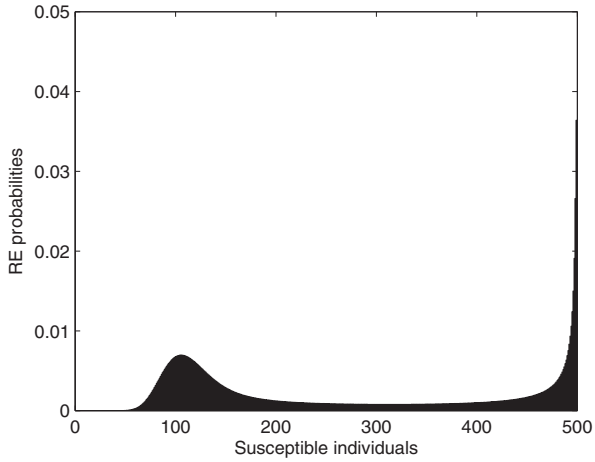

Fig. 7. RE mass function - *S* class.

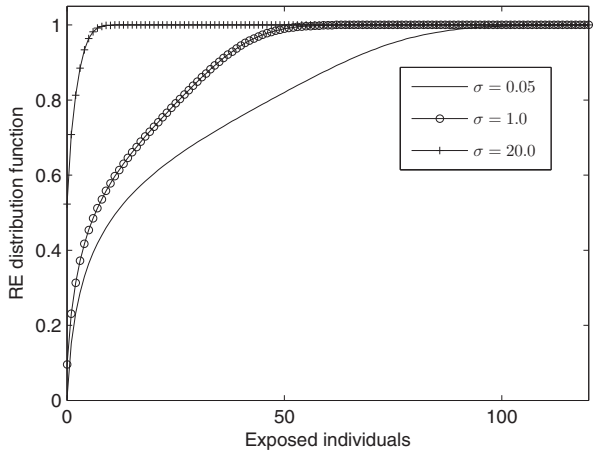

Fig. 8. RE distribution function - *E* class.

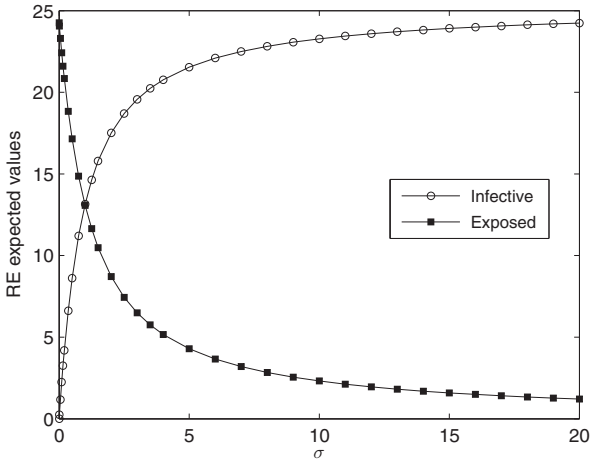

Fig. 9. RE mean values versus σ.

Table 3
Effect of the initial state.

(s_0, e_0, i_0)	$E[L(\infty)]$	$SD[L(\infty)]$	$E[D(\infty)]$	$SD[D(\infty)]$
S_a=(763,0,1)	77.45993	92.27595	171.39170	218.73362
S_b=(762,1,1)	123.48309	89.16898	276.76525	219.88370
S_c=(762,0,2)	119.70537	89.77132	276.76525	219.88370
S_d=(762,1,0)	83.90514	92.57836	170.49464	217.97737
S_e=(762,0,1)	77.40514	92.34989	170.49464	217.97737

- The RE probability mass functions for the removed and susceptible individuals may have a bimodal shape as well as the distributions of the final size and the extinction time.
- The latent rate σ is found to have negligible influence on the RE-distributions of the removed and susceptible individuals.

5.3. An application to Marburg fever 2005 outbreak in Angola

The 2005 outbreak of Marburg fever in Angola was the largest one reported to date with an extremely high mortality rate (about 91% compared to about 23% and 70% in previous outbreaks) and attacked disproportionately children under five years old. Indeed, the population of Angola is young (43.5% under 14) and with a high fertility (6.33 children per woman); thus it creates especially favorable conditions for the effective transmission and high mortality of the disease.

The causative agent of Marburg fever is a virus of the family *Filoviridae*, which also includes Ebola virus. Marburg fever symptoms are non-specific in their earlier stages and can be easily confused with other more common diseases such as malaria, yellow fever and typhoid fever. This is the main reason why an outbreak of the disease is usually confirmed after the occurrence of many fatal cases. This was also the case in the 2005 outbreak in Angola, where laboratory tests identified Marburg virus on March 23, 2005, in samples of 9 out of 12 fatal cases, whereas retrospective analysis at that time identified 102 cases (95 fatal), some of which dated back to October 2004 (see WHO report in [51]). This issue raises important difficulties in taking intervention measures in time and also in quantifying the spread of the epidemic in its initial stages.

In what follows, we apply some results derived in this paper to the study of the 2005 outbreak of Marburg fever in Angola. To this end, we use the statistical estimates obtained by Bettencourt [13], who studied a deterministic SEIR model of the same outbreak. More specifically, we adopt that $N = 764$, $\beta = 0.540$, $\gamma = 1/3$, $\sigma = 1/6.5$, while the mortality (i.e., the fraction of infected individuals that die from the disease) is taken to be $p = 0.910$. These model parameters provide our basic scenario along this section. The unit of time is a day.

First, we study the effect of the initial state on the expected extinction time, $E[L(\infty)]$, its standard deviation, $SD[L(\infty)]$, and the expected number of deaths, $E[D(\infty)] = pE[R(\infty)]$. The results are reported in Table 3, for the initial states $S_a = (763, 0, 1)$, $S_b = (762, 1, 1)$, $S_c = (762, 0, 2)$, $S_d = (762, 1, 0)$ and $S_e = (762, 0, 1)$. We observe the following numerical facts:

- The values of the expected number of deaths are equal in the scenarios S_b and S_c, as they are also equal in the scenarios S_d and S_e. This happens because the final size distribution of the epidemic depends only on the total number of initially affected individuals (infective and exposed), and not on the exact number of individuals in the E and I classes.
- In both scenarios S_d and S_e, the epidemic starts from one affected individual. The only difference is whether this individual is infected or exposed. In the latter case, it will take him an exponential time of $1/\sigma = 6.5$ days on average to become infective

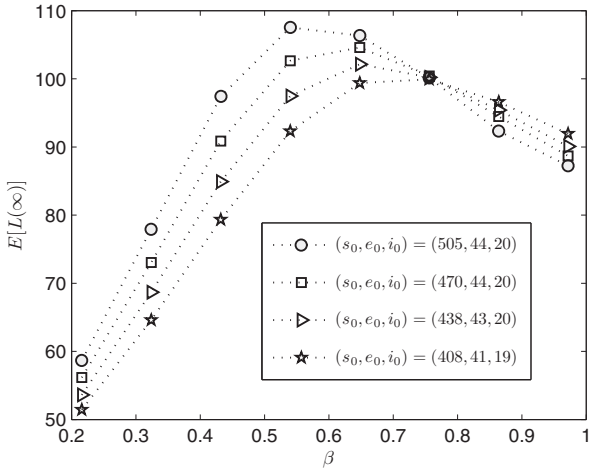

Fig. 10. Mean extinction time-Marburg data.

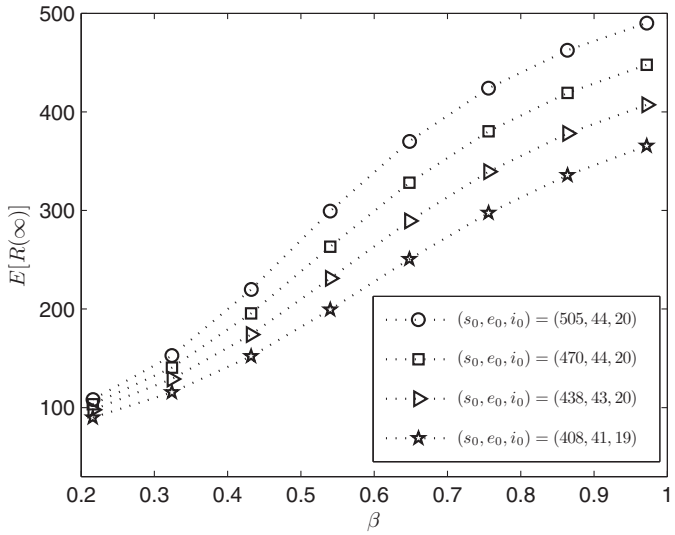

Fig. 11. Mean final size-Marburg data.

and then the epidemic will spread as if it had started with one infected individual. This justifies the differences in the expected values and standard deviations for the extinction time of the two scenarios.

- The scenario S_a contains one more susceptible than the scenario S_e, whereas they both start from one infected and no exposed individuals. The impact of this difference on the expected duration of the epidemic and the expected number of deaths is negligible.
- The scenarios S_a and S_c correspond to the same population size $N = 764$ and they have both 0 exposed individuals. However, S_c has two infected individuals, while S_a has only one. The impact of this apparently small change is particularly significant on both the expected duration of the epidemic and the expected number of deaths.
- Extinction times and number of deaths present similar concentration around its expected values in all the scenarios.

The biological implications that we gain from the above observations is that the final size distribution and the distribution of the extinction time are very sensitive to the initial number of affected individuals. Moreover, what matters most is the total number of affected individuals and not the exact number in each class. This conclusion shows that predictions should be taken very cautiously, as the number of exposed individuals is a hidden variable that cannot be observed.

In the second numerical experiment, we have drawn the graphs of the expected extinction time and the expected final size as functions of the contact rate β, for the initial states $S_1 = (505, 44, 20)$, $S_2 = (470, 44, 20)$, $S_3 = (438, 43, 20)$ and $S_4 = (408, 41, 19)$. These states are associated with the deterministic data obtained from the basic scenario on certain dates. For example, S_1 corresponds to April 4, the time at which an intervention of the health authorities starts, while S_4 corresponds to

April 19, after the time needed for the intervention to be implemented. The results are presented in Figs. 10 and 11 that enable the following observations:

- For a given initial state S_i, the corresponding curve allows us to see the effect of reducing the contact rate β. For example, in [13], the author describes that the initial contact rate $\beta = 0.540$ was cut by a factor of about 40% after an intervention of the health authorities. In other words, β was dropped from 0.540 to 0.324. This reduction of β implies a significant decrease from 299.281 to 152.578 on the expected final size (excluding the 195 initial removed individuals).
- For a fixed β, the consideration of various initial states S_i, which correspond to the epidemic state at different dates, show the effect of implementing the particular contact rate (by imposing an intervention measure) at one date rather than at another date. For example, for $\beta = 0.324$, if it was implemented on April 4 (i.e., we have S_1), then the approximate total number of cases of infection should be 348 (i.e., 152.57 + 195). On the other hand, if $\beta = 0.324$ is implemented two weeks later at April 19, then the approximate total number of cases of infection should be 412 cases.
- Fig. 10 shows that the expected extinction time, as a function of β, is unimodal, with a proper mode at a certain point $\beta_{\max}$. This may drive one to the false conclusion that for $\beta > \beta_{\max}$, the larger is β, the less aggressive is the epidemic. Of course, the contrary is true. As β becomes larger the epidemic becomes more aggressive and almost all individuals are infected immediately, so the expected duration of the epidemic decreases. Thus, the correct measure for the severity of the epidemic is not its mean duration but rather its final size; see also previous related comments in Subsection 5.2.

The main biological insight of this experiment is that a sensitivity analysis based on various possible contact rates β and initial states of an epidemic can enlighten our understanding of its spread. Moreover, it can be used to assess the possible gains of various interventions. Regarding the assessment of the severity of an epidemic, the message is that the mean final size is the crucial quantity and not the mean extinction time.

6. Conclusions

The contribution of this paper lies mainly in the elaboration of efficient computational procedures and algorithms for the study of the stochastic SEIR model. This is done by the consideration of two dual approaches, described in Sections 3 and 4, that compute the main descriptors of the model with reference to a fixed initial or target state, respectively. It should be emphasized that the two approaches are complementary and not alternatives of each other. The combination of them results in an effective computation of the main descriptors of the epidemic spread for populations of hundreds of individuals that correspond to state spaces with hundreds of millions states (see the relevant comments in Subsections 5.1, 5.2). These computational approaches have been checked to be more efficient than simulation for small and moderate population sizes (up to about 500 individuals). Having in mind that the stochastic approach is primarily concerned with the spread of epidemics in small populations, these algorithms may be used for the study of models with any size of practical interest, for which the stochastic approach is preferable.

From a theoretical point of view, the RE-distribution and the associated Little-type results shed light on the evolution of the number of infectives before extinction. The sensitivity of the duration of the epidemic with respect to the latent rate σ, in contrast to the insensitivity of the final size distribution clarify the similarities and the differences between the stochastic SIR and SEIR models. It seems fair to say that the SIR and SEIR models have similar behavior regarding the RE distributions, but differ significantly regarding the extinction time distribution. In this sense, the use of the SEIR model, rather than the corresponding SIR model, seems necessary when one considers issues associated with the duration of an outbreak.

Regarding biological–epidemiological insight, the effect of the length of the latent periods on the evolution of the epidemic has been illuminated. Moreover, the sensitivity of the behavior of the epidemic on the initial number of affected individuals and on the basic reproduction ratio $\mathcal{R}_0$ has been shown to be particularly significant. Indeed, Whittle's [49] famous threshold theorem states that for a stochastic *SIR* model the probability of a major outbreak is approximately $1 - (1/\mathcal{R}_0)^i$, when $I(0) = i$, for $\mathcal{R}_0 > 1$. This result applies also to the SEIR model with $E(0) = 0$, $I(0) = i$, it justifies the bimodality of the final size, and also the bimodality of the extinction time and the RE-distributions that was observed in our numerical experiments.

The study would be continued in various directions. In particular, it seems important to investigate further the effect of the latent periods on the spread of a stochastic epidemic. In this sense, it is important to relax the exponentiality assumption on the underlying latent periods. Another problem of interest is the study of stochastic SEIR models in populations with heterogeneities. Finally, the consideration of models in which individuals pass through more stages of infectivity seems also a challenging problem, since the number of states of the underlying Markov chains explodes rapidly. Nevertheless, the consideration of such models is important as they represent more accurately the evolution of various diseases.

Acknowledgments

This work was supported by the Government of Spain (Department of Science and Innovation) and the European Commission through project MTM 2011–23864. M.J. Lopez-Herrero is a member of the "Stochastic Modelling Group - UCM910211", which was supported by the Complutense University of Madrid and Banco de Santander, call 2014-GR3/14. We would like also to note that the first author of this work, J.R. Artalejo, passed away suddenly a few weeks after the completion of the first version of this paper. His memory will stay with us for ever.

Appendix A. The infinitesimal generator Q

We next show the structure of the infinitesimal generator $\mathbf{Q}$ with infinitesimal transition rates (2). The state space S can be partitioned as $S = \cup_{s=0}^{N-1} l_s$, where l_s is the s-th level of the process that contains the states with $S(t) = s$. Each level l_s is partitioned in sub-levels as $l_s = \cup_{e=0}^{N-s-1} l_{se}$, where l_{se} is the (s, e)-th sublevel of the process that contains the states with $(S(t), E(t)) = (s, e)$. Then, we are able to express the infinitesimal generator $\mathbf{Q}$ in the block lower triangular form

$$\mathbf{Q} = \begin{pmatrix} \mathbf{Q}_{00} & \mathbf{0} & \mathbf{0} & \cdots & \mathbf{0} & \mathbf{0} & \mathbf{0} \\ \mathbf{Q}_{10} & \mathbf{Q}_{11} & \mathbf{0} & \cdots & \mathbf{0} & \mathbf{0} & \mathbf{0} \\ & \ddots & \ddots & \ddots & \ddots & \ddots & \\ \mathbf{0} & \mathbf{0} & \mathbf{0} & \cdots & \mathbf{Q}_{N-2,N-3} & \mathbf{Q}_{N-2,N-2} & \mathbf{0} \\ \mathbf{0} & \mathbf{0} & \mathbf{0} & \cdots & \mathbf{0} & \mathbf{Q}_{N-1,N-2} & \mathbf{Q}_{N-1,N-1} \end{pmatrix},$$

where the blocks $\mathbf{Q}_{ss'}$ are of dimension $|l_s| \times |l_{s'}|$ and $\mathbf{0}$ is a matrix of zeros. Partitioning the blocks $\mathbf{Q}_{ss'}$ according sub-levels, we have

$$\mathbf{Q}_{s,s-1} = \begin{pmatrix} \mathbf{0} & \mathbf{Q}_{(s,0)(s-1,1)} & \mathbf{0} & \cdots & \mathbf{0} & \mathbf{0} \\ \mathbf{0} & \mathbf{0} & \mathbf{Q}_{(s,1)(s-1,2)} & \cdots & \mathbf{0} & \mathbf{0} \\ & \ddots & \ddots & \ddots & \ddots & \\ \mathbf{0} & \mathbf{0} & \mathbf{0} & \cdots & \mathbf{0} & \mathbf{Q}_{(s,N-s-1)(s-1,N-s)} \end{pmatrix},$$

for $1 \le s \le N-1$, and

$$\mathbf{Q}_{ss} = \begin{pmatrix} \mathbf{Q}_{(s,0)(s,0)} & \mathbf{0} & \mathbf{0} & \cdots & \mathbf{0} & \mathbf{0} \\ \mathbf{Q}_{(s,1)(s,0)} & \mathbf{Q}_{(s,1)(s,1)} & \mathbf{0} & \cdots & \mathbf{0} & \mathbf{0} \\ & \ddots & \ddots & \ddots & \ddots & \\ \mathbf{0} & \mathbf{0} & \mathbf{0} & \cdots & \mathbf{Q}_{(s,N-s-1)(s,N-s-2)} & \mathbf{Q}_{(s,N-s-1)(s,N-s-1)} \end{pmatrix},$$

for $0 \le s \le N-1$. The non-zero sub-blocks $\mathbf{Q}_{(s,e)(s-1,e+1)}$ contain rates that correspond to transmission of the disease to susceptible individuals, whereas $\mathbf{Q}_{(s,e)(s,e-1)}$ provide rates that correspond to completions of latent periods. On the other hand the sub-blocks $\mathbf{Q}_{(s,e)(s,e)}$ contain rates that correspond to recoveries of infective individuals. Moreover, these sub-blocks also give the diagonal rates $-q_{sei}$. More specifically, we have

$$\mathbf{Q}_{(s,e)(s-1,e+1)} = \begin{pmatrix} \beta_{s0} & 0 & 0 & \cdots & 0 & 0 \\ 0 & \beta_{s1} & 0 & \cdots & 0 & 0 \\ & \ddots & \ddots & \ddots & \ddots & \\ 0 & 0 & 0 & \cdots & \beta_{s,N-s-e-1} & 0 \\ 0 & 0 & 0 & \cdots & 0 & \beta_{s,N-s-e} \end{pmatrix},$$

for $1 \le s \le N-1$ and $0 \le e \le N-s-1$,

$$\mathbf{Q}_{(s,e)(s,e-1)} = \begin{pmatrix} 0 & \sigma_e & 0 & \cdots & 0 & 0 \\ 0 & 0 & \sigma_e & \cdots & 0 & 0 \\ & \ddots & \ddots & \ddots & \ddots & \\ 0 & 0 & 0 & \cdots & \sigma_e & 0 \\ 0 & 0 & 0 & \cdots & 0 & \sigma_e \end{pmatrix},$$

for $0 \le s \le N-1$ and $1 \le e \le N-s-1$, and

$$\mathbf{Q}_{(s,e)(s,e)} = \begin{pmatrix} -q_{se0} & 0 & 0 & \cdots & 0 & 0 & 0 \\ \gamma_1 & -q_{se1} & 0 & \cdots & 0 & 0 & 0 \\ & \ddots & \ddots & \ddots & \ddots & \ddots & \\ 0 & 0 & 0 & \cdots & \gamma_{N-s-e-1} & -q_{se,N-s-e-1} & 0 \\ 0 & 0 & 0 & \cdots & 0 & \gamma_{N-s-e} & -q_{se,N-s-e} \end{pmatrix},$$

for $0 \le s \le N-1$ and $0 \le e \le N-s-1$.

Appendix B. Symbolic inversion of the LST of the extinction time

Since the infinitesimal generator $\mathbf{Q}$ of X is triangular, its eigenvalues are the diagonal rates $-q_{sei}$, with $q_{sei} = \frac{\beta}{N} si + \sigma e + \gamma i$. For $i = 0$, we have that $q_{se0} = \sigma e$ independently of the value of s, so we have the set of 'natural' multiple eigenvalues $\{-\sigma e : \ 1 \le e \le N-2\}$, where the eigenvalue $-\sigma e$ corresponds to the states $\{(s, e, 0) : \ 0 \le s \le N-1-e\}$; hence it has algebraic multiplicity $N-e$, for $1 \le e \le N-2$.

Some 'casual' multiple eigenvalues may also exist, in case where some parameters assume special values. For example, in the case $N = 3$, any of the conditions $\gamma = \sigma$, $3\gamma = \sigma$, $\frac{\beta}{N} + \gamma = \sigma$ or $2\frac{\beta}{N} + \gamma = 2\sigma$ implies the existence of additional multiple eigenvalues with multiplicity 2. However, in practice these cases do not arise, as the validity of such conditions is artificial and has negligible probability in reality. So, in what follows, we assume that the rates $\frac{\beta}{N}$, γ and σ are linearly independent elements of the vector space $\mathbb{R}$ of the real numbers with coefficients from the field $\mathbb{Q}$ of the rational numbers. This assumption is not restrictive from a practical viewpoint and allows us to conclude that the only multiple eigenvalues are the natural ones. A partial fraction decomposition [36] reduces the recursive Eq. (8) for $\varphi_{sei}(z)$, for $(s, e, i) \in S_T$, to the form

$$\begin{aligned}\varphi_{sei}(z) &= \frac{P_{sei}(z)}{\prod_{(s',e',i')\le(s,e,i)}(z+q_{s'e'i'})} \\ &= \sum_{(s',e',i')\le(s,e,i)} \delta_{l^{(s,e,i)}_{(s',e',i')},1} A_{(s,e,i)}(s',e',i') \frac{q_{s'e'i'}}{z+q_{s'e'i'}} \\ &\quad + \sum_{(s',e',i')\le(s,e,i)} (1-\delta_{l^{(s,e,i)}_{(s',e',i')},1}) \sum_{n=1}^{l^{(s,e,i)}_{(s',e',i')}} A^n_{(s,e,i)}(s',e',i') \left(\frac{q_{s'e'i'}}{z+q_{s'e'i'}}\right)^n, \end{aligned} \tag{11}$$

where $P_{sei}(z)$ is a polynomial of z, $A_{(s,e,i)}(s', e', i')$ and $A^n_{(s,e,i)}(s', e', i')$ are coefficients to be determined below, and $l^{(s,e,i)}_{(s',e',i')}$ is the multiplicity of $q_{s'e'i'}$ referred to the subset $\{q_{s''e''i''} : (s'', e'', i'') \le (s, e, i)\}$.

The coefficients can be recursively computed in the natural order (see Section 3). In particular, $A_{(s,e,i)}(s', e', i')$ can be evaluated as $A_{(s,e,i)}(s', e', i') = \frac{1}{q_{s'e'i'}} \lim_{z\to -q_{s'e'i'}} (z + q_{s'e'i'})\varphi_{sei}(z)$. We distinguish the following two cases:

Case I: $(s', e', i') < (s, e, i)$ and $l^{(s,e,i)}_{(s',e',i')} = 1$. Then

$$A_{(s,e,i)}(s', e', i') = \frac{1}{q_{sei} - q_{s'e'i'}} \sum_{(s'',e'',i'')_T \ge (s',e',i')} q_{(s,e,i)(s'',e'',i'')} A_{(s'',e'',i'')}(s', e', i'),$$

where the notation $(s'', e'', i'')_T$ indicates that the sum refers only to transient states.

Case II: $(s', e', i') = (s, e, i)$ and $l^{(s,e,i)}_{(s',e',i')} = 1$. Then

$$A_{(s,e,i)}(s, e, i) = \frac{1}{q_{sei}} \left(\sum_{(s'',e'',i'')_T < (s,e,i)} q_{(s,e,i)(s'',e'',i'')} B_{(s,e,i)}(s'', e'', i'') + \sum_{(s'',e'',i'')_A < (s,e,i)} q_{(s,e,i)(s'',e'',i'')} \right),$$

where $(s'', e'', i'')_A$ denotes that the sum is over absorbing states and

$$\begin{aligned} B_{(s,e,i)}(s'', e'', i'') &= \sum_{(s',e',i')\le(s'',e'',i'')} \delta_{l^{(s'',e'',i'')}_{(s',e',i')},1} A_{(s'',e'',i'')}(s', e', i') \frac{q_{s'e'i'}}{q_{s'e'i'} - q_{sei}} \\ &\quad + \sum_{(s',e',i')\le(s'',e'',i'')} (1-\delta_{l^{(s'',e'',i'')}_{(s',e',i')},1}) \sum_{n=1}^{l^{(s'',e'',i'')}_{(s',e',i')}} A^n_{(s'',e'',i'')}(s', e', i') \left(\frac{q_{s'e'i'}}{q_{s'e'i'} - q_{sei}}\right)^n. \end{aligned}$$

On the other hand, the coefficients $A^n_{(s,e,i)}(s', e', i')$ are associated with the following case:

Case III: $(s', e', i') < (s, e, i)$ and $l^{(s,e,i)}_{(s',e',i')} > 1$. Let N_{sei} be the total number of unknown coefficients associated with the state (s, e, i) (i.e., N_{sei} is obtained by adding the multiplicities $l^{(s,e,i)}_{(s',e',i')} > 1$ along the states (s', e', i') strictly smaller than (s, e, i)). Then, we evaluate $\varphi_{sei}(z)$ at N_{sei} different points that do not belong to the set of eigenvalues of the matrix $\mathbf{Q}$ (so as no denominator is 0 in (11)). In this way, we obtain a linear system of equations whose solution gives the N_{sei} desired coefficients.

Note that $l^{(s,e,i)}_{(s,e,i)} = 1$, so the above three cases are exhaustive. After computing the coefficients $A_{(s,e,i)}(s', e', i')$ and $A^n_{(s,e,i)}(s', e', i')$, we can then symbolically invert (11), by recognizing that $(\frac{q_{sei}}{z+q_{sei}})^n$ is the LST corresponding to an Erlang random variable with parameters q_{sei} and n . The probability density functions $f_{sei}(t)$ of the remaining extinction time, given the current state $(s, e, i) \in S_T$, are given as

$$\begin{aligned} f_{sei}(t) &= \sum_{(s',e',i')\le(s,e,i)} \delta_{l^{(s,e,i)}_{(s',e',i')},1} A_{(s,e,i)}(s', e', i') q_{s'e'i'} e^{-q_{s'e'i'}t} \\ &\quad + \sum_{(s',e',i')\le(s,e,i)} (1-\delta_{l^{(s,e,i)}_{(s',e',i')},1}) \sum_{n=1}^{l^{(s,e,i)}_{(s',e',i')}} A^n_{(s,e,i)}(s', e', i') \frac{q^n_{s'e'i'}}{(n-1)!} t^{n-1} e^{-q_{s'e'i'}t}. \end{aligned}$$

References

[1] J. Abate, W. Whitt, Numerical inversion of Laplace transforms of probability distributions, ORSA J. Comput. 7 (1995) 36–43.
[2] L.J.S. Allen, Anintroduction to stochastic epidemic models, Lecture Notes in Mathematics, 1945, Springer, Berlin, 2008, pp. 81–130.
[3] L.J.S. Allen, E.J. Allen, A comparison of three different stochastic population models with regard to persistence time, Theor. Popul. Biol. 64 (2003) 439–449.

[4] H. Andersson, T. Britton, Stochastic epidemic models and their statistical analysis, Lecture Notes in Statistics, 151, Springer, New York, 2000.
[5] H. Anton, C. Rorres, Elementary Linear Algebra, Applications version, 10th, Anton Textbooks Inc., 2010.
[6] J.R. Artalejo, A. Economou, M.J. Lopez-Herrero, Stochastic epidemic models revisited: analysis of some continuous performance measures, J. Biol. Dyn. 6 (2012) 189–211.
[7] J.R. Artalejo, A. Economou, M.J. Lopez-Herrero, Stochastic epidemic models with random environment: quasi-stationarity, extinction and final size, J. Math. Biol. 67 (2013) 799–831.
[8] J.R. Artalejo, M.J. Lopez-Herrero, Quasi-stationarity and ratio of expectations distributions: a comparative study, J. Theor. Biol. 266 (2010) 264–274.
[9] F. Ball, A unified approach to the distribution of the total size and total area under the trajectory of infectives in epidemic models, Adv. Appl. Prob. 18 (1986) 289–310.
[10] F. Ball, P.D. O'Neill, J. Pike, Stochastic epidemic models in structured populations featuring dynamic vaccination and isolation, J. Appl. Prob. 44 (2007) 571–585.
[11] A.D. Barbour, P.K. Pollett, Total variation approximation for quasi-stationary distributions, J. Appl. Prob. 47 (2010) 934–946.
[12] M.S. Bartlett, Deterministic and stochastic models for recurrent epidemics, in: J. Neyman (Ed.), Biology and Problems of Health, IV, 1956, pp. 81–109. Proceedings of the 3rd Berkeley Symposium on Mathematical Statistics and Probability
[13] L.M.A. Bettencourt, C. Castillo-Chavez, An ensemble trajectory method for real-time modeling and prediction of unfolding epidemics: analysis of the 2005 Marburg fever outbreak in Angola, in: G. Chowell, J.M. Hyman, L.M.A. Bettencourt, C. Castillo-Chavez (Eds.), Mathematical and Statistical Estimation Approaches in Epidemiology., Springer, New York, 2009, pp. 143–161.
[14] A.J. Black, J.V. Ross, Computation of epidemic final size distributions, J. Theor. Biol. 367 (2015) 159–165.
[15] T. Britton, Stochastic epidemic models: a survey, Math. Biosci. 225 (2010) 24–35.
[16] G. ChowellJ. HymanL. BettencourtC. Castillo-Chavez (Eds.), Mathematical and Statistical Estimation Approaches in Epidemiology, Springer, New York, 2009.
[17] D.J. Daley, J. Gani, Epidemic Modelling: An Introduction, Cambridge Studies in Mathematical Biology, 15, Cambridge University Press, Cambridge, 1999.
[18] J.N. Darroch, E. Seneta, On quasi-stationary distributions in absorbing continuous-time finite Markov chains, J. Appl. Prob. 4 (1967) 192–196.
[19] J.N. Darroch, E. Seneta, On quasi-stationary distributions in absorbing discrete-time finite Markov chains, J. Appl. Prob. 2 (1965) 88–100.
[20] M. De la Sen, S. Alonso-Quesada, A simple vaccination control strategy for the SEIR epidemic model, in: Proceedings of the 2010 IEEE ICMIT, 2010, pp. 1037–1044.
[21] P.P.G. Dyke, An Introduction to Laplace Transforms and Fourier Series, Springer, London, 2000.
[22] W.J. Ewens, The pseudo-transient distribution and its uses in genetics, J. Appl. Prob. 1 (1964) 141–156.
[23] D.T. Gillespie, A general methodology for numerically simulating the stochastic time evolution of coupled chemical reactions, J. Comput. Phys. 22 (1976) 403–434.
[24] D.T. Gillespie, Exact stochastic simulation of coupled chemical reactions, J. Phys. Chem. 81 (1977) 2340–2361.
[25] N.S. Goel, N. Richter-Dyn, Stochastic Models in Biology, Academic Press, New York, 1974.
[26] J. Goyens, J. Reijniers, B. Borremans, H. Leirs, Density thresholds for Mopeia virus invasion and persistence in its host Mastomys natalensis, J. Theor. Biol. 317 (2013) 55–61.
[27] J. Grasman, Stochastic epidemics: the expected duration of the endemic period in higher dimensional models, Math. Biosci. 152 (1998) 13–27.
[28] C. Groendyke, D. Welch, D.R. Hunter, Bayesian inference for contact networks given epidemic data, Scand. J. Stat. 38 (2011) 600–616.
[29] L.K. Hotta, Bayesian melding estimation of a stochastic SEIR model, Math. Popul. Stud. 17 (2010) 101–111.
[30] T. House, J.V. Ross, D. Sirl, How big is an outbreak likely to be? Methods for epidemic final-size calculation, P. R. Soc. A - Math. Phys. 469 (2013) 20120436.
[31] J.A. Jacquez, C.P. Simon, The stochastic SI model with recruitment and deaths I. Comparison with the closed SIS model, Math. Biosci. 117 (1993) 77–125.
[32] M.J. Keeling, P. Rohani, Modeling Infectious Diseases in Humans and Animals, Princeton University Press, Princeton, New Jersey, 2008.
[33] M.J. Keeling, J.V. Ross, On methods for studying stochastic disease dynamics, J. R. Soc. Interface 5 (2008) 171–181.
[34] W.O. Kermack, A.G. McKendrick, A contribution to the mathematical theory of epidemics, Proc. R. Soc. Lond. A 115 (1927) 700–721.
[35] A. Korobeinikov, Global properties of SIR and SEIR epidemic models with multiple parallel infectious stages, Bull. Math. Biol. 71 (2009) 75–83.
[36] V.G. Kulkarni, Modeling and Analysis of Stochastic Systems, Chapman and Hall, London, 1995.
[37] Y.A. Kuznetsov, C. Piccardi, Bifurcation analysis of periodic SEIR and SIR epidemic models, J. Math. Biol. 32 (1994) 109–121.
[38] M.Y. Li, H.L. Smith, L. Wang, Global dynamics of an SEIR epidemic model with vertical transmission, SIAM J. Appl. Math. 62 (2001) 58–69.
[39] J.D.C. Little, A proof of the queueing formula $L = \lambda W$, Oper. Res. 9 (1961) 383–387.
[40] M.F. Neuts, J.-M. Li, An algorithmic study of S-I-R Stochastic epidemic models, in: C.C. Heyde, Yu V. Prohorov, R. Pyke, S.T. Rachev (Eds.), Athens Conference on Applied Probability and Time Series, 1, Springer-Verlag, Heidelberg, 1996, pp. 295–306.
[41] R.H. Norden, On the distribution of the time to extinction in the stochastic logistic population model, Adv. Appl. Prob. 14 (1982) 687–708.
[42] I.B. Schwartz, H.L. Smith, Infinite subharmonic bifurcation in an SEIR epidemic model, J. Math. Biol. 18 (1983) 233–253.
[43] S.E.F. Spencer, P.D. O'Neill, Assessing the impact of intervention delays on stochastic epidemics, Methodol. Comput. Appl. Prob. 13 (2013) 803–820.
[44] P. Stone, H. Wilkinson-Herbots, V. Isham, A stochastic model for head lice infections, J. Math. Biol. 56 (2008) 743–763.
[45] A. Svensson, On the asymptotic size and duration of a class of epidemic models, J. Appl. Prob. 32 (1995) 11–24.
[46] J. Swinton, Extinction times and phase transitions for spatially structured closed epidemics, Bull. Math. Biol. 60 (1998) 215–230.
[47] E.A. van Doorn, P.K. Pollett, Survival in quasi-death process, Linear Algebra Appl. 429 (2008) 776–791.
[48] E.A. van Doorn, P.K. Pollett, Quasi-stationary distributions for discrete-state models, Eur. J. Oper. Res. 230 (2013) 1–14.
[49] P. Whittle, The outcome of a stochastic epidemic - a note on Bailey's paper, Biometrika 42 (1955) 116–122.
[50] D.J. Wilkinson, Stochastic Modelling for Systems Biology, 2nd, CRC Press, Taylor & Francis Group, Boca Raton, Florida, 2012.
[51] World Health Organization Outbreak updates, http://www.who.int/csr/don/archive/disease/marburg_virus_disease/en/index.html.